Polymer Actuators Using Ion−Gel Electrolytes Prepared by Self-Assembly of ABA-Triblock Copolymers

ARTICLE *in* MACROMOLECULES · JANUARY 2012

Impact Factor: 5.8 · DOI: 10.1021/ma2022138

3 AUTHORS, INCLUDING:

Masayoshi Watanabe
Yokohama National University
350 PUBLICATIONS **14,344** CITATIONS

SEE PROFILE

Macromolecules

Article

pubs.acs.org/Macromolecules

Polymer Actuators Using Ion-Gel Electrolytes Prepared by Self-Assembly of ABA-Triblock Copolymers

Satoru Imaizumi, Hisashi Kokubo, and Masayoshi Watanabe*

Department of Chemistry and Biotechnology, Yokohama National University, Tokiwadai, Hodogaya-ku, Yokohama 240-8501, Japan

Supporting Information

ABSTRACT: Well-defined ABA-triblock copolymers, polystyrene-*block*-poly(methyl methacrylate)-*block*-polystyrene (SMS), which have two different polystyrene (PSt) weight fractions (f_{PSt}), were synthesized by successive atom-transfer radical polymerizations. Ion gels consisting of SMS and an ionic liquid, (1-ethyl-3-methylimidazolium bis(trifluoromethanesulfonyl)amide [C_2mim][NTf_2]), were prepared using the cosolvent evaporation method with tetrahydrofuran. Atomic force microscope images of the ion gels indicated that PSt is phase-separated to form sphere domains that serve as physical cross-linking points because PSt is not compatible with [C_2mim][NTf_2], while a continuous poly(methyl methacrylate) (PMMA) phase with dissolved [C_2mim][NTf_2] is formed to serve as ion conduction paths. Accordingly, the ion gels are formed by the self-assembly of SMS and the preferential dissolution of [C_2mim][NTf_2] into the PMMA phase. The viscoelastic properties of the gels can be easily controlled by changing f_{PSt} in SMS and [C_2mim][NTf_2] concentration in the ion gels. The ion gels that exhibit high ionic conductivities (>10^{-3} S cm^{-1}) at room temperature were used as an electrolyte of an ionic polymer actuator, which has a trilaminar structure consisting of the ion-gel electrolyte sandwiched between two composite carbon electrodes containing high-surface-area activated carbon powders. By applying low voltages (<3.0 V) to the electrodes, the actuator exhibited a soft bending motion toward the anodic side.

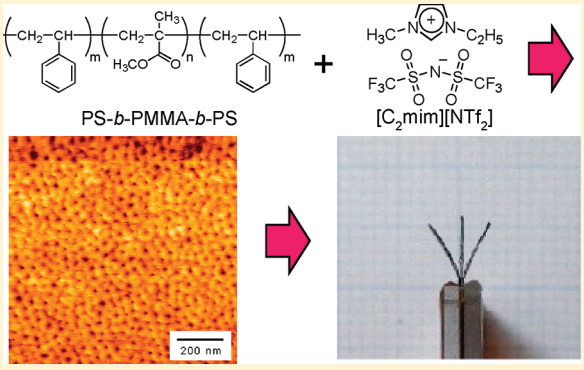

1. INTRODUCTION

Ionic liquids (ILs) exhibit unique properties such as thermal and (electro)chemical stability, nonvolatility, nonflammability, and high ionic conductivity; consequently, they have been an area of intense interest.[1] ILs have received much attention since Wilkes et al. reported air- and water-stable ILs containing the tetrafluoroborate anion in 1992.[2] ILs are generally regarded as environmentally benign green solvents and a promising class of functional materials. The properties of ILs can be adjusted widely because an infinite number of possible combinations of cations and anions can be achieved. For this reason, ILs are sometimes referred to as "designer solvents" and "third solvents" following water and organic solvents.

From the standpoint of materials science, the combination of ILs and polymers is promising for the development of novel materials because certain polymers are compatible with ILs.[3−5] The development of polymer electrolytes with unique properties such as thin-film formability, flexibility, and transparency in addition to high ionic conductivity has been an intensive topic of many researchers attempting to realize novel electrochemical devices.[6] In 1993, we published the first report on a polymer electrolyte containing an IL with an exceptionally high ionic conductivity.[7] This electrolyte was molecular composites consisting of a chloroaluminate IL and a polymer. Subsequently, we found that common vinyl monomers are widely soluble in air- and water-stable ILs and that they can be polymerized in ILs by free-radical polymerization.[8] In certain cases, good compatibility of the resulting polymers with the ILs can be achieved, regardless of the polymer concentration and temperature. Network polymers containing ILs (ion gels) can be obtained in such cases.[8] During the same time as our above research, many other studies investigated the solidification or gelation of ILs to obtain solid electrolytes by utilizing crystalline fluorinated copolymers,[9] stereocomplex formations of poly(methyl methacrylate)s,[10] and self-organization of amphiphilic block copolymers,[11] as well as the addition of colloidal nanoparticles[12−14] and low molecular weight gelators.[15,16] Among them, the utilization of block copolymers is of great interest since this methodology may have the potential to afford easily processable and mechanically strong ion gels by utilizing self-assembly of the block copolymers. Lodge et al. have been conducting systematic studies of the preparation, structure, rheology, and application of ions gels consisting of block copolymers and ILs.[11,17]

Applicable fields of ion gels are diverse, e.g., solid electrolytes of electrochemical devices such as capacitors,[18] batteries,[19] fuel cells,[20] solar cells,[21] and actuators;[22−24] membranes for gas separation[25] and catalytic reactions;[26] and dielectric layers of

Received: October 3, 2011
Revised: November 25, 2011
Published: December 15, 2011

Scheme 1. Synthesis of SMSs by Successive ATRPs

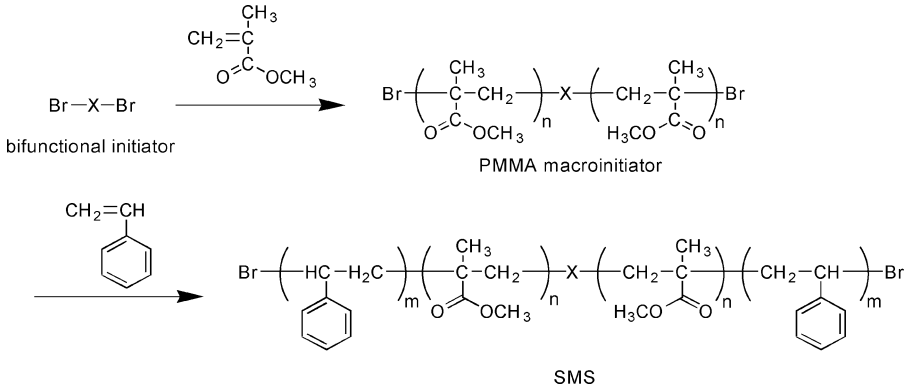

organic transistors.[27] We have been especially interested in polymer actuators as an application of ion gels. As a material for manufacturing artificial muscles with biomimetic soft motion, polymer actuators using electroactive polymer (EAP) have been applied to manipulators and robotic devices.[28−32] Ionic EAP actuators[30−32] driven by diffusion or migration of ions can exhibit relatively large deformation in response to application of low voltages. However, these actuators have a serious problem with regard to their durability under atmospheric conditions owing to evaporation of solvents, which are necessary to provide environments that permit the movement of ions. To overcome such problems, ILs have been applied to the electrolytes of ionic EAPs.[22−24] Most research in this field has focused on optimization of the electrolytes by changing the IL structures,[33] but very few studies have focused on matrix polymers for ILs. Indeed, poly(vinylidene fluoride-*co*-hexafluoropropylene) (P(VDF-*co*-HFP))[24,33a−d] and Nafion[23,33e] have been mainly investigated in this context. Thus, additional knowledge regarding the effects of the polymer structure and properties on the performance of actuators is needed.

In this study, we investigated the microstructures, rheological properties, and ionic conductivity of ion gels formed by self-assembly of polystyrene-*block*-poly(methyl methacrylate)-*block*-polystyrene (SMS) triblock copolymers,[11c] prepared by successive atom-transfer radical polymerizations (ATRP).[34,35] Our previous study showed that polystyrene (PSt) and poly(methyl methacrylate) (PMMA) were insoluble and soluble, respectively, in 1-ethyl-3-methylimidazolium bis(trifluoromethanesulfonyl)amide ([C_2mim][NTf_2]);[36] thus, preferential dissolution of [C_2mim][NTf_2] in the PMMA phase was expected, which was also confirmed by the study by Frisbie and Lodge et al.[11c] The continuous PMMA phase with dissolved [C_2mim][NTf_2] may serve as conduction paths for the IL, while the phase-separated PSt phase may serve as physical cross-linking points. Furthermore, we report the performance of the polymer actuators using ion-gel electrolytes consisting of SMS and [C_2mim][NTf_2]. Chemically deposited noble-metal electrodes[23,30] and carbon nanotubes,[24,37] have been widely used as electrode materials for ionic EAPs. We have proposed that inexpensive and ubiquitous carbon materials such as activated carbon can be used as electrode material of the actuators.[38] Here, we demonstrate an ionic EAP actuator with a trilamellar structure consisting of an ion-gel electrolyte sandwiched between two composite carbon electrodes containing high-surface-area activated carbon powders. The correlation between the actuator performance and the properties of the ion gels is also discussed.

2. EXPERIMENTAL SECTION

Materials. An ionic liquid, [C_2mim][NTf_2], was prepared according to the literature with slight modification[39] and dried under vacuum at 100 °C for 24 h. The water content in [C_2mim][NTf_2] determined by Karl Fischer titration was less than 10 ppm. 2-Bromoisobutyl bromide, dehydrated anisole, and 4,4′-dinonyl-2,2′-bipyridine (dNbpy) were purchased from Aldrich and used without further purification. CuBr and $CuBr_2$ were purchased from Wako Chemical. CuBr was washed with glacial acetic acid, dehydrated ethanol, and diethyl ether, dried under vacuum, and then stored in an argon-atmosphere glovebox (VAC). $CuBr_2$ was dried under vacuum and stored in the same drybox. Ethylene glycol, triethylamine and *N*,*N*,*N*′,*N*′,*N*″-pentamethyldiethylenetriamine (PMDETA) were purchased from Tokyo Chemical Industry, and were dried by molecular sieves. Methyl methacrylate (MMA) and styrene (both from Wako Chemical) were dried by calcium hydride overnight and vacuum-distilled prior to use.

Synthesis of a Bifunctional Initiator. A bifunctional initiator, ethylene glycol bis(2-bromoisobutyrate), was synthesized according to the literature.[40] To accomplish this, ethylene glycol (5.6 mL, 0.10 mol) and triethylamine (34 mL, 0.24 mol) were dissolved in 300 mL of diethyl ether in a three-necked flask under a N_2 atmosphere, after which the solution was cooled to 0 °C in an ice bath. Next, 2-bromoisobutyl bromide (30 mL, 0.24 mol) was dropped into the solution, and the solution was stirred overnight. The reaction solution was then filtered, after which the filtrate was washed with water three times. Finally, white needle crystals (14 g, 39 mmol, yield 39%) were obtained by recrystallization from ethanol/H_2O. ^{1}H NMR of the bifunctional initiator (400 MHz, $CDCl_3$): δ (ppm) = 1.94 (s, $(CH_3)_2C$, 12H), 4.44 (s, OCH_2, 4H). (The spectrum is shown in Supporting Information, Figure S-1)

Synthesis of PMMA Macroinitiator. The bifunctional initiator (1.7 g, 4.8 mmol) and $CuBr_2$ (2.5 mg, 0.24 mmol) were dried under reduced pressure in a three-necked flask. Anisole (200 mL) and PMDETA (0.63 μL, 3.0 mmol) were then added to the flask. To dissolve $CuBr_2$ by complex formation with PMDETA, the solution was stirred overnight at 60 °C under a N_2 atmosphere. After cooling the solution, CuBr (0.34 mg, 2.4 mmol) and MMA (200 mL, 1.9 mol) were added to the flask. The reaction mixture was then degassed by sonication under reduced pressure and successive N_2 replacement three times. A polymerization reaction was subsequently conducted at 60 °C for 6 h with stirring (Scheme 1). Next, the reaction was quenched by cooling to 0 °C, after which the crude polymer was isolated by precipitation into an excess amount of methanol and collected by suction filtration. The polymer was then dissolved again in ethyl acetate and the solution was purified by column chromatography (alumina) to remove the Cu complexes from the PMMA. The eluted ethyl acetate solution of the PMMA was poured into a large excess of hexane, and the precipitates were filtered and dried under vacuum. The purified PMMA macroinitiator was obtained as white powder (Yield: 90 g). The molecular characterization results are shown in Table 1.

dx.doi.org/10.1021/ma2022138 | *Macromolecules* 2012, 45, 401−409

Table 1. Monomer Conversion, Molecular Weight, Molecular Weight Distribution, and Composition of PMMA and SMSs

	convn[a]	$M_{n,theo}$ ($\times 10^{-4}$)[b]	M_n ($\times 10^{-4}$)	M_w/M_n[c]	f_{PSt} (wt %)[d]
PMMA[e]	0.47[f]	1.9	1.89[c]	1.12	–
SMS-18	0.1[g]	2	2.31[f]	1.11	18.3[f]
SMS-48	0.3[g]	4	3.65[f]	1.16	48.2[f]

[a]Monomer conversion. [b]Calculated from monomer conversion. [c]Evaluated by GPC analysis using PMMA standard. [d]Weight fraction of PSt in the SMS. [e]Utilized as a macroinitiator for SMSs. [f]Calculated by ^{1}H NMR analysis. [g]Calculated from polymer yield.

Synthesis of ABA-Triblock Copolymers. The synthesized PMMA macroinitiator (20 g, 1.1 mmol), CuBr (0.13 g, 0.87 mmol), $CuBr_2$ (5.8 mg, 0.026 mmol), and dNbpy (0.76 g, 1.9 mmol) were added into a dried round-bottom flask. Styrene (80 mL, 0.69 mol), which is not only a monomer but also a reaction solvent, was then poured into the flask. The polymerization reaction was then allowed to proceed at 100 °C. At 26 and 45 h from the initiation of the polymerization, heating was stopped. The obtained polymer was then isolated and purified by reprecipitation using a similar method as that used for the PMMA macroinitiator. The weight fractions of PSt in SMS-18 and SMS-48 were evaluated from ^{1}H NMR spectra shown in Figure S-2, Supporting Information. The molecular characterization results of the block copolymers are shown in Table 1. Gel permeation chromatograms (GPC) of the PMMA macroinitiator and ABA-triblock copolymers (Figure 1) indicated that well-defined block copolymers were prepared by the successive ATRP method.

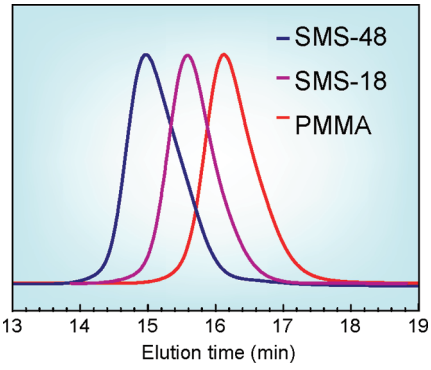

Figure 1. Gel permeation chromatograms of PMMA macroinitiator and SMS block copolymers.

Material Characterization. Viscoelastic measurements were conducted using a Physica MCR301 (Anton Paar) rotary rheometer with an H-PTD200 temperature controller. A parallel plate (25 or 50 mm diameter) was installed, depending on the modulus of each sample. The frequency dispersion was measured in the frequency range of 0.1 to 100 rad s^{-1} and in the temperature range from 120 to 0 °C by 10 °C steps. The samples were thermally equilibrated at each temperature for at least 1 h before the measurements. Differential scanning calorimetry (DSC) was conducted using a Seiko Instruments DSC 6220 under a nitrogen atmosphere. The samples were tightly sealed in aluminum pans in the dry glovebox. The DSC measurements were conducted by heating to +150 °C, cooling to −150 °C, and then heating to +150 °C at a cooling and heating rate of 10 °C min^{-1}. The glass transition temperatures (T_g) were determined from the mid points of heat capacity changes in the DSC thermograms during the programmed reheating scans. Atomic force microscope (AFM) images were recorded at room temperature by an SPA-400 microscope unit and a SPI3800N probe controller (Seiko Instruments Inc.) in tapping mode, using a silicon cantilever with a spring constant of 15 N m^{-1}. A lump of the ion gel sample was frozen with liquid N_2, cleaved, and sliced into a thin film to expose the cleaved face for the AFM observation. The ionic conductivity of the ion gels was determined from complex impedance measurements using a Hewlett-Packard 4192A LF impedance analyzer over a frequency range of 5 Hz to 13 MHz. The ion gel samples were then placed between two stainless steel disk electrodes separated by a polytetrafluoroethylene spacer with an inner diameter of 8.5 mm and a height of 3 mm. The cell constant was determined using a 0.01 M KCl standard aqueous solution. The sample cell was placed in a thermo-regulated bath and thermally equilibrated at each temperature for at least 1 h before taking the measurements.

Preparation and Measurement of Ion Gel Actuators. Preweighed amounts of SMS and $[C_2mim][NTf_2]$ were dissolved in tetrahydrofuran (THF) as a cosolvent. After casting the THF solution in a flat Petri dish, the THF was gradually removed from the solution at ambient temperatures and then dried under vacuum for more than 12 h. Transparent and flexible ion gel membranes (SMS/$[C_2mim][NTf_2]$ composites) were obtained by this procedure.

Ion gel actuators have a trilaminar structure consisting of an ion-gel electrolyte membrane sandwiched between two carbon electrodes. The carbon electrodes were prepared by mixing activated carbon (24 wt %, Kuraray Co. Ltd.), Ketjen black (3 wt %, Lion Corp.), P(VDF-*co*-HFP) (8 wt %, Arkema Inc.), and $[C_2mim][NTf_2]$(65 wt %) using a conditioning mixer (AR-250, Thinky). The mixture was then hot pressed with a polyimide spacer (50 μm) at 130 °C. Next, ion gel membranes with a thickness of 100 μm were fabricated by hot pressing at 130−160 °C, and the electrode membranes were attached to both sides of the ion-gel electrolyte by hot pressing at 80−130 °C to fabricate a monolithic trilaminar membrane. The thickness of the actuators became a little thinner (ca. 10 μm) than the total thickness of the electrodes and the electrolyte by the final hot pressing. Rectangular pieces (width of 2 mm and length of 7 mm) were cut from the monolithic membrane and clipped between Cu tapes connected to a potentiostat (HA-301, Hokuto Denko) and a function generator (HB-104, Hokuto Denko). Displacement of the actuator was measured at room temperature by a laser displacement meter (LC-2440, Keyence) at 4 mm from the clamped end.

3. RESULTS AND DISCUSSION

Formation of Ion Gels. It is interesting to explore how effectively $[C_2mim][NTf_2]$ gelates with the addition of SMS block copolymers. The gelation point of the SMS and $[C_2mim][NTf_2]$ binary systems was evaluated by dynamic viscoelastic measurement. The dynamic rheological properties measured under a constant strain amplitude within a linear viscoelastic regime are shown in Figure 2. The 7 wt % dispersions are liquids for both SMS block copolymer systems; the viscous modulus (G'') exceeds the elastic modulus (G') over the entire frequency range, and both moduli exhibit dependence on frequency. The dispersions show a complicated response at 9 wt % for SMS-18 and at 8 wt % for SMS-48. Specifically, the moduli exhibit a crossover at a high frequency. However, G' is dominant and the moduli become relatively independent of frequency toward the low end of the frequency spectrum. At 9 wt % for SMS-48, G' is larger than G'' and becomes less dependent on frequency over the entire measured range. These findings indicate that dispersions containing greater than 9 wt % for SMS-18 and more than 8 wt % for SMS-48 behave as soft solid materials (ion gels). In appearance, binary systems containing SMS at levels just below the gelation concentrations were bluish viscous liquids because of Rayleigh scattering, and these systems became extremely viscous as they approached gelation. Binary systems containing SMS at levels higher than the gelation concentrations became transparent and colorless gels.

dx.doi.org/10.1021/ma2022138 | *Macromolecules* 2012, 45, 401−409

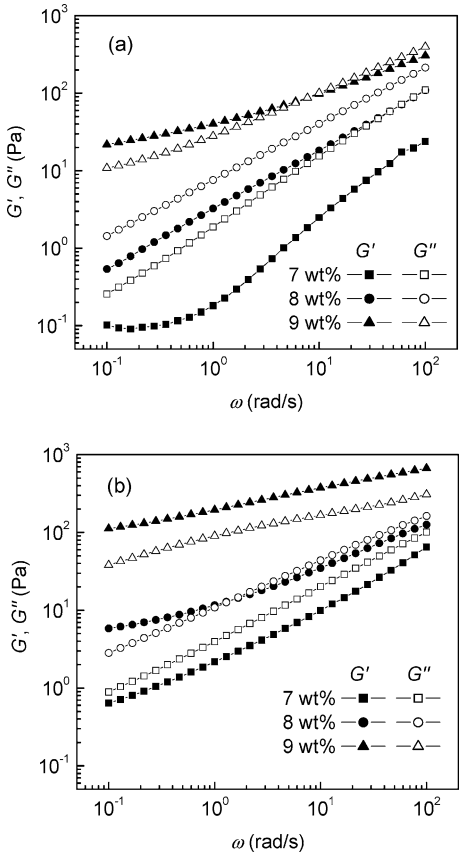

Figure 2. Storage (G') and loss (G'') moduli as a function of frequency for binary systems consisting of $[C_2mim][NTf_2]$ and SMS-18 (a) or SMS-48 (b) at 20 °C.

Lodge et al. reported that gelation of an IL, 1-butyl-3-methylimidazolium hexafluorophosphate ($[C_4mim]PF_6$), could be achieved by the self-assembly of as little as 5 wt % of a triblock copolymer, PSt-*block*-poly(ethylene oxide)(PEO)-*block*-PSt (SOS), where M_n of the each terminal PSt is 4760 Da, M_n of the middle PEO is 25 500 Da, the polydispersity index (M_w/M_n) is 1.36, and the PSt weight fraction (f_{PSt}) is 0.28.[11a] Although there are differences in the IL-philic segment structure; PEO against PMMA, and in the IL structures; $[C_4mim]PF_6$ against $[C_2mim][NTf_2]$, the critical gelation concentrations of these block copolymers are comparable. The somewhat lower gelation concentration of SOS than that of SMS may be ascribed to its higher M_n of the IL-philic PEO segment. They also recently reported physical properties of $[C_2mim][NTf_2]$ ion-gels with the 10 wt % addition of an SMS block copolymer (M_n of the SMS = 121 kDa, f_{PSt} = 0.29).[11c]

Figure 3 shows the viscoelastic moduli (G' and G'') of the ion gels containing 10 wt % SMSs as a function of temperature in the range of 0 to 120 °C at a frequency of 1 rad/s. The SMS-18 ion gel exhibits a crossing of G' and G'' at around 50 °C, where the sol−gel transition occurs. This sol−gel transition temperature is almost the same as T_g of PSt (= ca. 50 °C) with molecular weight of 2 kDa,[41] however, it depends on the angular frequency, as shown in Figure S-3, Supporting Information. SMS concentrations also affect the sol−gel transition temperatures (Figure S-4, Supporting Information). These results indicate that the stability of PSt cross-linking points cannot be explained only by the magnitude of T_g. The higher is the concentration or angular frequency, the higher

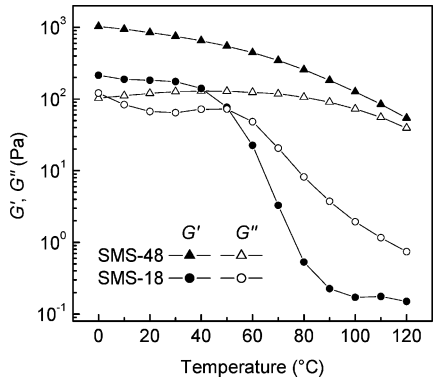

Figure 3. Temperature dependence of G' and G'' of ion gels based on SMS-48 (10 wt %) and SMS-18 (10 wt %) at 1 rad/s.

appears the sol−gel transition temperature. Conversely, the SMS-48 ion gel displays no transition over the measured temperature (0−120 °C). This phenomenon indicates that the PSt domain remains aggregated even above its T_g (=ca. 90 °C) with molecular weight of 9 kDa,[41] because PSt is less compatible with $[C_2mim][NTf_2]$. The difference in the sol−gel transition behavior of SMS-18 and SMS-48 appears to be caused by the difference in the incompatibility between PSt and $[C_2mim][NTf_2]$, which strongly depends on the molecular weight of PSt blocks. Strain dependencies of the viscoelastic moduli are shown in Figure 4. A linear regime was maintained

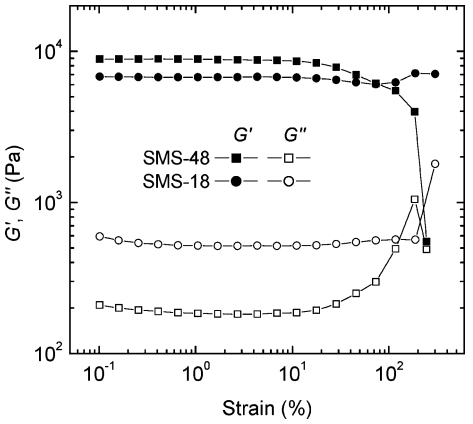

Figure 4. G' and G'' as a function of strain for ion gels containing 15 wt % of SMS-18 or SMS-48 at 25 °C and 1 Hz.

for up to 10% strain for each ion gel. By applying larger strain, the polymer networks were broken, possibly because of slipping-off of PSt chains from PSt domains that serve as physical cross-linking points of the ion gels. The plateau G' of the SMS-18 composite and SMS-48 composite are 7 and 9 kPa, respectively. The higher tan δ (=G''/G') value of the SMS-18 composite than that of the SMS-48 composite suggests that the number of looped chains, which are dominant in the sol state and ineffective in the formation of the gels, remains in a larger quantity in the SMS-18 composite. This is supported by the fact that deviation from the G' values of ideal gels is larger for SMS-18 than that for SMS-48 (Figure S-5, Supporting Information). The ion gel formed by SMS-48 has a higher cross-linking density than that formed by SMS-18, resulting in a hard and brittle gel.

dx.doi.org/10.1021/ma2022138 | *Macromolecules* 2012, 45, 401−409

Microstructure and Ionic Conductivity of Ion Gels. To confirm selective dissolution of $[C_2mim][NTf_2]$ in PMMA segments, which was expected from the observations in the rheological measurements (*vide supra*), we conducted DSC measurements of the ion gels. The DSC thermograms for SMS-48/$[C_2mim][NTf_2]$ are shown in Figure S-6, Supporting Information. The T_g values and the transition widths determined from the onsets and ends of heat capacity changes are listed in Table S-1, Supporting Information. Figure 5 shows

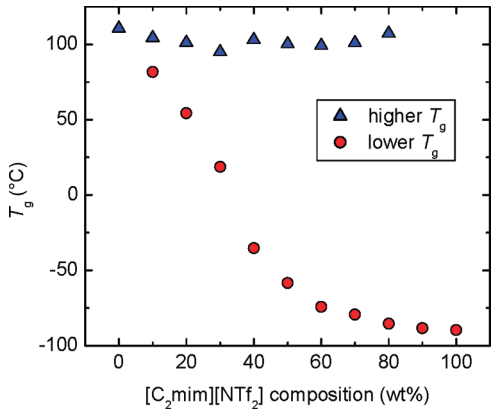

Figure 5. T_g of ion gels based on SMS-48 as a function of weight fraction of $[C_2mim][NTf_2]$.

the T_g values of ion gels based on SMS-48 plotted against $[C_2mim][NTf_2]$ weight fractions. In the case of neat SMS-48, only one T_g is observed at ca. 100 °C. We can not distinguish T_g values of PSt and PMMA because they are close together. As the weight fraction of $[C_2mim][NTf_2]$ increases, one T_g is still retained at ca. 100 °C, whereas another T_g appears at lower temperatures. In $[C_2mim][NTf_2]$ composition range of 30−50 wt %, the heat capacity changes corresponding to the lower T_gs are broadened (Figure S-6 and Table S-1, Supporting Information). Lodge et al. recently reported that PMMA/$[C_2mim][NTf_2]$ solutions have two apparent glass transitions at intermediate compositions, even if the binary systems are good solvent solutions.[42] We also observed similar phenomena in the network PMMA with dissolved $[C_2mim][NTf_2]$.[8b,c] In the present case, the broadening may also be caused by the coexistence of PMMA-rich region and $[C_2mim][NTf_2]$-rich region. When the weight fraction of $[C_2mim][NTf_2]$ becomes higher than 0.8, T_g at ca. 100 °C disappears and only one T_g appears at low temperature. When the weight fraction of $[C_2mim][NTf_2]$ becomes high, T_g of PSt cannot be observed because of a small heat capacity change accompanied by glass transition of PSt.

Figure 6 shows a tapping-mode AFM phase image of an ion gel containing 30 wt % of SMS-48. In this image, the bright region indicates a softer and more attractive surface, while the dark region indicates a harder and less-attractive surface. As expected, the image clearly shows that the ion gel is phase-separated between soft and hard domains.[43] The continuous bright portions and spherical dark portions correspond to PMMA(15 wt %) with dissolved $[C_2mim][NTf_2]$(70 wt %) domains and PSt(15 wt %) domains, respectively. In this case, the PSt spheres did not appear to form a fully ordered structure from the AFM image. Figure S-7 (Supporting Information) shows a two-dimensional (2D) Fourier power spectrum corresponding to the AFM image (Figure 6). An obscurely

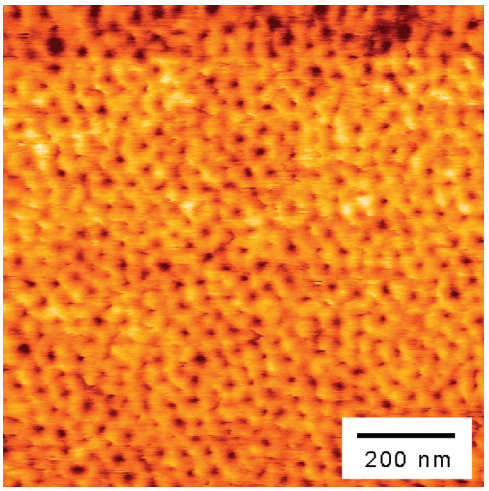

Figure 6. Tapping-mode AFM phase image of an ion gel based on SMS-48 (30 wt %).

ring-shaped 2D Fourier power spectrum is obtained, which indicates that the microphase separated structure of the ion gel does not have a fully ordered cubic structure, but rather a short-range ordered structure. Since phase diagram of block copolymers is well understood,[43] it is interesting to know the factors that determine the phase behavior and ordered/disordered structures. In the case of ordinary block copolymers, the ordered/disordered structures depend on the compatibility and segment size of each block.[43] Strongly segregated systems with less compatible blocks with large segment size take ordered structures. In the present case, quantitative compatibility of $[C_2mim][NTf_2]$ with PMMA and further that between PSt and PMMA with dissolved $[C_2mim][NTf_2]$ remains unexplored at a fundamental level.[5b] We just speculate now that the segregation between PSt and PMMA with dissolved $[C_2mim][NTf_2]$ is not strong enough to form a fully ordered structure.

Figure 7 shows the Arrhenius plot of ionic conductivities for the ion gels. The conductivity values were calculated from a cell

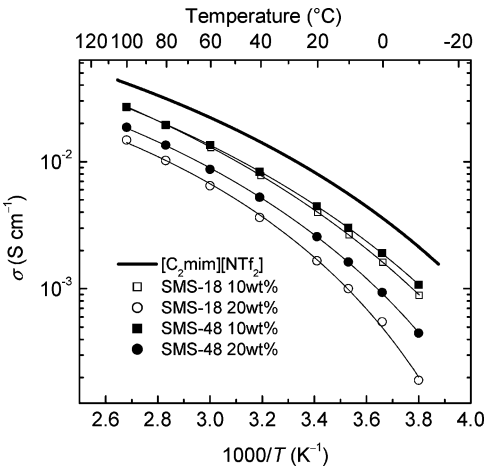

Figure 7. Arrhenius plots of ionic conductivity for the ion gels based on the SMS block copolymers with dissolved $[C_2mim][NTf_2]$.

constant and the real part of cell impedance value (Z') where the imaginary part of cell impedance ($-Z''$) takes a minimum in the Nyquist plots (Z' vs $-Z''$ plots). Typical Nyquist plots are

dx.doi.org/10.1021/ma2022138 | *Macromolecules* 2012, 45, 401−409

as shown in Figure S-8, Supporting Information, which consist of a low frequency spur corresponding to the interfacial impedance and a high frequency arc corresponding to the bulk impedance. There were no significant changes in the shape of the Nyquist plots with temperature, polymer concentration, and f_{PS} of SMS. Room temperature ionic conductivities of the gels reach 10^{-3} S cm^{-1}, and the temperature dependencies can be represented by the Vogel–Fulcher–Tammann (VFT) equation. On the basis of the VFT equation and the best-fit parameters (Supporting Information, Table S-2), the lines on the plots reproduce the experimental data well. It is also interesting to note that the ion gel based on SMS-18 exhibits continuous conductivities expressed by the VFT equation from −10 to +100 °C, even though the binary system undergoes a sol–gel transition at ca. 50 °C, as shown in Figure 3. This is contrasted by the previous observation that gel electrolytes based on ABA block copolymers, polyethylene-*block*-poly(ethylene oxide-*co*-propylene oxide)-*block*-polyethylene, and a 1 M Li[NTf$_2$] solution in γ-butyrolactone.[44] The gel electrolytes exhibit discontinuous conductivity changes at the sol–gel transition temperatures owing to melting of the end-polyethylene-blocks. In this case, there should be certain interactions between the Li salts and the midpolyether-blocks, which result in discontinuous conductivity increases at gel-to-sol transitions owing to melting of the end-blocks. Conversely, the [C$_2$mim][NTf$_2$] consists of extremely weak Lewis acidic cations and Lewis basic anions.[45] Thus, the motion of [C$_2$mim][NTf$_2$] is relatively decoupled from the motion of PMMA segments,[8c] and the melting of end-PSt-blocks does not contribute to acceleration of the transport of [C$_2$mim][NTf$_2$].

The ionic conductivities of the SMS-48 ion gels are higher than those of SMS-18 ion gels at the same block copolymer compositions. Since we have reported the ionic conductivities of loosely cross-linked PMMA networks with dissolved [C$_2$mim][NTf$_2$],[8b] we simulated the ionic conductivities of SMS ion gels based on a two-phase model composed of continuous PMMA domains with dissolved [C$_2$mim][NTf$_2$] and isolated PSt domains. This two-phase model assumes complete phase separation between these two phases. The conductivity can be written as

$$\sigma = \phi\sigma(\text{PMMA} + [\text{C}_2\text{mim}][\text{NTf}_2]) + (1 - \phi)\sigma(\text{PSt})$$

where ϕ is the volume fraction of the PMMA domains with dissolved [C$_2$mim][NTf$_2$]. Because of the negligibly low conductivity of σ(PSt), the above equation can be rewritten as

$$\sigma = \phi\sigma(\text{PMMA} + [\text{C}_2\text{mim}][\text{NTf}_2])$$

The broken lines in Figure 8 show σ(PMMA + [C$_2$mim][NTf$_2$]) determined from our data,[8b] and the solid lines represent ϕ σ(PMMA + [C$_2$mim][NTf$_2$]). Both of these values are plotted against the weight fraction of SMS in the ion gels. As shown in the figure, the ϕ (volume fraction of the PMMA/[C$_2$mim][NTf$_2$]) has little effect on the σ values. The experimental data shown by solid plots are reasonably located along the solid lines, and interference of the ion transport by the PSt domains appears to be very small. The higher conductivity for the SMS-48 ion gels than the SMS-18 ion gels shown in Figure 7 simply comes from the fact that the PMMA phase in the SMS-48 ion gel contains larger amounts of [C$_2$mim][NTf$_2$] at the same SMS weight fraction and thus exhibits higher σ(PMMA + [C$_2$mim][NTf$_2$]). This effect overwhelms the small ϕ for the SMS-48 ion gels. Since the ionic diffusion of [C$_2$mim][NTf$_2$] is interrupted by the

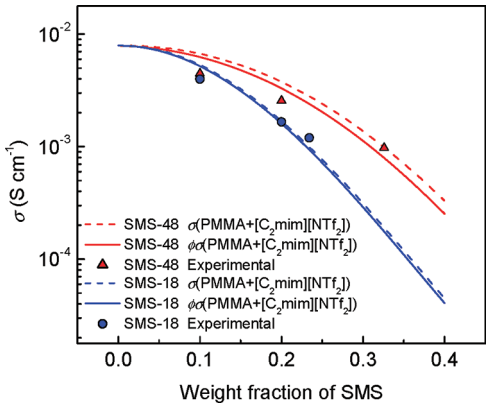

Figure 8. Ionic conductivity at 20 °C as a function of weight fraction of SMS for the ion gels containing [C$_2$mim][NTf$_2$]. Broken line: σ(PMMA + [C$_2$mim][NTf$_2$]) from ref8b; Solid line: ϕ σ(PMMA +[C$_2$mim][NTf$_2$]). Solid plots: experimental data.

interaction with PMMA chains,[8b] the ionic mobility is mainly determined by the PMMA/[C$_2$mim][NTf$_2$] compositions.

Performance of Polymer Actuator Using Ion Gels. The self-assembly of the SMS block copolymers in an IL was shown to form highly ion-conductive and nonvolatile soft-materials (ion gels). Here, we show an application of the ion gels to ionic EAP actuators. Figure 9 shows the current and bending

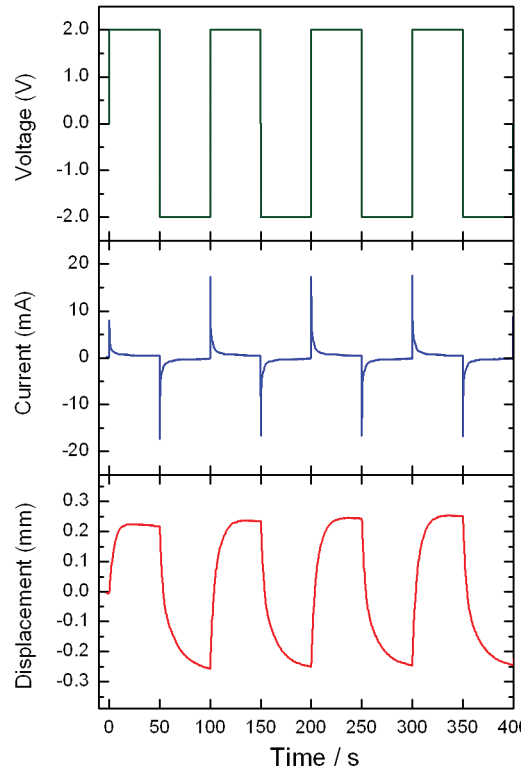

Figure 9. Current and displacement responses of an ion gel actuator based on SMS-18 (20 wt %) against application of ±2.0 V rectangular voltage with a cycle of 100 s.

displacement responses of an ion gel actuator against a rectangular voltage application (see also Figure S-9, Supporting Information). When voltage is applied to the actuator, charging current is observed, but this current decays exponentially with time. No faradaic current was observed in the cyclic

dx.doi.org/10.1021/ma2022138 | *Macromolecules* 2012, 45, 401–409

voltammetry within the voltage range of ±2.0 V. These phenomena indicate that charging and discharging of the electric double layer formed at the interface between the activated carbon and $[C_2mim][NTf_2]$ in the electrode layer is responsible for displacement of the actuator. It should be noted that the bending displacement is always directed toward the anodic side. In other words, the actuator bends toward the positively polarized electrode direction. This behavior has been widely observed in ionic EAP actuators using ILs.[23,24,33,46] We have investigated the transport properties of common ionic liquids in detail, especially imidazolium-based ILs.[47] Interestingly, the diffusivity of the cations is larger than that of anions in most cases, even if the van der Waals radius of the cations is larger than that of the anion.[47c] Typically, the cationic and anionic diffusivity of $[C_2mim][NTf_2]$ is clarified to be 4.4×10^{-7} and 2.5×10^{-7} cm^2 s^{-1}, respectively, at 20 °C,[47c] which corresponds to a cationic transference number of 0.64. The cationic transference number in the PMMA-based ion gels also becomes larger as the mole fraction of $[C_2mim][NTf_2]$ decreases (increasing the mole fraction of PMMA) owing to preferential interaction of the $[NTf_2]$ anion with PMMA chains.[8b] Such imbalanced transport between the cation and anion induces concentration polarization of $[C_2mim][NTf_2]$ inside the polymers (PMMA in the electrolyte layer and P(VDF-*co*-HFP) in the electrode layer) via electrochemical polarization of the actuators. On the anodic side, the concentration becomes lower than that in the bulk, while on the cathodic side, it becomes larger than that in the bulk. This concentration polarization causes swelling of the cathodic electrode layer and deswelling of the anodic electrode layer, which appears to explain such displacement. The actuation mechanism will be discussed in detail in a forthcoming paper.

The applied voltage dependence of the displacement of the ion gel actuators is shown in Figure 10. As the applied voltages

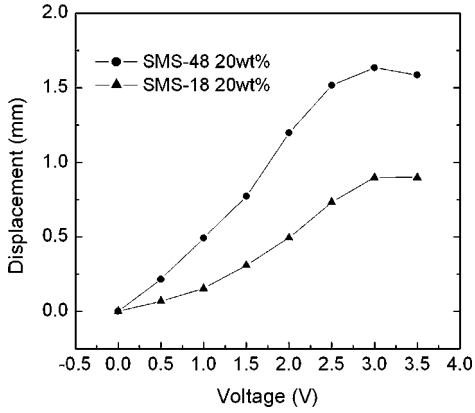

Figure 10. Displacement of ion gel actuators based on SMS block copolymers as a function of the magnitude of rectangular-wave voltages at a cycle of 100 s.

increase, electric charges stored in the electric double layer increase, resulting in an increase in displacement up to ca. 1.6 mm at 3.0 V, which is 40% of its length. However, when a voltage of 3.5 V is applied, the displacement does not change or decreases slightly, despite an increase in the flowing current. Reversibility of motion of the actuators also deteriorated at an applied voltage of 3.5 V. This is due to certain irreversible faradaic reactions. Although the electrochemical potential window $[C_2mim][NTf_2]$ is reported to be wider than 4 V,[39,48] the actuator experiments were conducted under atmospheric conditions and the contamination by water and oxygen could cause to reduce the electrochemical stability of the actuator. Figure 11 shows the displacement amplitude of

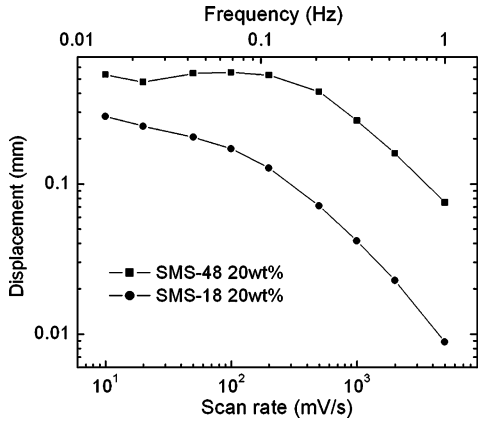

Figure 11. Scan rate dependence of the displacement amplitude for ion gel actuators based on SMS block copolymers with the application of ±1.5 V triangular wave voltage.

the actuators with the application of ±1.5 V triangular wave voltage as a function of the scan rate and a function of the frequency (upper horizontal axis). The actuator based on SMS-48 demonstrates superior performance in terms of displacement amplitude and speed. These results reflect the difference in the electrolyte properties. Specifically, the ionic conductivities of the ion gels containing 20 wt % of SMS-48 and SMS-18 at 20 °C are 2.4×10^{-3} and 1.7×10^{-3} S cm^{-1}, respectively. Higher conductivity makes the time constants of the actuators smaller, which enhances the amount of electricity stored at the electric double layers and the magnitude of concentration polarization of $[C_2mim][NTf_2]$ at a constant voltage scan rate. The simplest equivalent circuit for the actuators is the series connection of a resistance and a capacitance. The resistance (R) correlates with the conductivity and shape of ion gels and the capacitance (C) corresponds to the double layer capacitance between the ion gel and carbon electrodes. Actual R and C values of the actuator were estimated to be R = 40 Ω and C = 0.1 F for an ion gel actuator based on SMS-18 (20 wt %), which is shown in Figure 9. In this case, the time constant becomes 4 s. However, the displacement in Figure 9 continues to increase for several tens of seconds. In the actuation experiments, one end of a rectangular trilaminar-specimen was clipped between Cu current-collectors. The carbon electrode layer is much more resistive compared with the metal. Consequently, the potential drop along longitudinal direction of the actuator specimen cannot be neglected. This is the main reason why the time constant of the actuator during actuation becomes longer than that estimated from the R and C values. However, for fast and large movement of the actuators, reduction of the time constant by the achievement of high ionic conductivity of the ions gels and large double-layer capacitance as well as the achievement of high electronic conductivity of the carbon electrodes appears to be the most crucial requirements.

■ CONCLUSION

We investigated the gelation of an IL, $[C_2mim][NTf_2]$, by self-assembly of SMS block copolymers. The rheological properties, AFM images, and ionic conductivity of the SMS/$[C_2mim]$-

dx.doi.org/10.1021/ma2022138 | *Macromolecules* 2012, 45, 401–409

[NTf_2] binary systems are reasonable if we assume that the gelation occurs via aggregation of the PSt segments in the IL owing to incompatibility with [C_2mim][NTf_2] and that the resulting ion gels have two-phase structures consisting of continuous PMMA phases with preferentially dissolved [C_2mim][NTf_2] and isolated PSt phases. The aggregated PSt phases serve as physical cross-linking points of the ion gels.

Moreover, we fabricated ionic EAP actuators using SMS/[C_2mim][NTf_2] ion gels. The ion gel actuators have a trilaminar structure composed of the ion-gel electrolyte sandwiched between two composite carbon electrodes containing high-surface-area activated carbon powders. By applying low voltages (<3.0 V) to the electrodes, the actuator exhibited soft bending motion toward the anodic side. The displacement of the actuator increased with an increase in the charge stored at the electric double layer between the activated carbon and the IL, eventually increasing to 40% of its length. The ionic conductivity of the ion gels was closely correlated with the performance of the actuators.

■ ASSOCIATED CONTENT

Supporting Information

Characterization of materials (Figure S-1 and S-2), rheological properties (Figure S-3, S-4, and S-5), thermal properties (Table S-1 and Figure S-6), two-dimensional Fourier power spectrum of a tapping mode AFM phase image (Figure S-7), ionic conductivity (Figure S-8 and Table S-2), and photographs of the movement of an ion gel actuator (Figure S-9). This material is available free of charge via the Internet at http://pubs.acs.org.

■ AUTHOR INFORMATION

Corresponding Author

*Telephone and fax: +81-45-339-3955. E-mail: mwatanab@ynu.ac.jp.

■ ACKNOWLEDGMENTS

This work was supported in part by Grants-in-aid for Scientific Research on Priority Areas (No. 438-19016014 and No. 452-17073009) from the MEXT of Japan.

■ REFERENCES

(1) (a) Welton, T. *Chem. Rev.* **1999**, *99*, 2071. (b) Holbrey, J. D.; Seddon, K. R. *Clean Prod. Process* **1999**, *1*, 223. (c) Wasserscheid, P.; Keim, W. *Angew. Chem., Int. Ed.* **2000**, *39*, 3772. (d) Wilkes, J. S. *Green Chem.* **2002**, *4*, 73. (e) Seddon, K. R. *Nat. Mater.* **2003**, *2*, 363. (f) Plechkova, N. V.; Seddon, K. R. *Chem. Soc. Rev.* **2008**, *37*, 123.

(2) Wilkes, J. S.; Zaworotko, M. J. *J. Chem. Soc., Chem. Commun.* **1992**, 965.

(3) *Ionic liquids in Polymer Systems: Solvents, Additives, and Novel Applications*; ACS Symposium Series 913; Brazel, C. S., Rogers, R. D., Eds.; American Chemical Society: Washington DC, 2005.

(4) Winterton, N. *J. Mater. Chem.* **2006**, *16*, 4281.

(5) (a) Ueki, T.; Watanabe, M. *Macromolecules* **2008**, *41*, 3739. (b) Ueki, T.; Watanabe, M. *Bull. Chem. Soc. Jpn.* **2011**, DOI: 10.1246/bcsj.20110225.

(6) (a) *Polymer Electrolyte Reviews 1 and 2*; MacCallum, J. R., Vincent, C. A., Eds.; Elsevier: London, 1987 and 1989. (b) Gray, F. M. *Solid Polymer Electrolytes*; VCH Publishers: New York, 1991. (c) *Application of Electroactive Polymers*; Scrosati, B., Ed.; Chapman & Hall: London, 1993.

(7) Watanabe, M.; Yamada,, S.-I.; Sanui, K.; Ogata, N. *J. Chem. Soc., Chem. Commun.* **1993**, 929.

(8) (a) Noda, A.; Watanabe, M. *Electrochim. Acta* **2000**, *45*, 1265. (b) Susan, M. A. B. H.; Kaneko, T.; Noda, A.; Watanabe, M. *J. Am. Chem. Soc.* **2005**, *127*, 4976. (c) Seki, S.; Susan, M. A. B. H.; Kaneko, T.; Tokuda, H.; Noda, A.; Watanabe, M. *J. Phys. Chem. B* **2005**, *109*, 3886.

(9) (a) Carlin, R. T.; Fuller, J. *Chem. Commun.* **1997**, 1345. (b) Fuller, J.; Breda, A. C.; Carlin, R. T. *J. Electrochem. Soc.* **1997**, *144*, L67. (c) Fuller, J.; Breda, A. C.; Carlin, R. T. *J. Electroanal. Chem.* **1998**, *459*, 29.

(10) Kawauchi, T.; Kumaki, J.; Okoshi, K.; Yashima, E. *Macromolecules* **2005**, *38*, 9155.

(11) (a) He, Y.; Boswell, P. G.; Bühlmann, P.; Lodge, T. P. *J. Phys. Chem. B* **2007**, *111*, 4645. (b) Lodge, T. P. *Science* **2008**, *321*, 50. (c) Zhang, S.; Lee, K. H.; Frisbie, C. D.; Lodge, T. P. *Macromolecules* **2011**, *44*, 940.

(12) (a) Hasegawa, K.; Tatsumisago, M.; Minami, T. *J. Electrochem. Soc.* **1999**, *146*, 3359. (b) Wang, P.; Zakeeruddin, S. M.; Comte, P.; Exner, I.; Grätzel, M. *J. Am. Chem. Soc.* **2003**, *125*, 1166. (c) Usui, H.; Matusi, H.; Tanabe, N.; Yanagida, S. *J. Photochem. Photobiol. A* **2004**, *164*, 97. (d) Katakabe, T.; Kawano, R.; Watanabe, M. *Electrochem. Solid-State Lett.* **2007**, *10*, F23.

(13) (a) Ueno, K.; Inaba, A.; Kondoh, M.; Watanabe, M. *Langmuir* **2008**, *24*, 5253. (b) Ueno, K.; Hata, K.; Katakabe, T.; Kondoh, M.; Watanabe, M. *J. Phys. Chem. B* **2008**, *112*, 9013. (c) Ueno, K.; Imaizumi, S.; Hata, K.; Watanabe, M. *Langmuir* **2009**, *25*, 825. (d) Ueno, K.; Inaba, A.; Sano, Y.; Kondoh, M.; Watanabe, M. *Chem. Commun.* **2009**, 3603. (e) Ueno, K.; Sano, Y.; Inaba, A.; Kondoh, M.; Watanabe, M. *J. Phys.Chem. B* **2010**, *114*, 13095. (e) Ueno, K.; Watanabe, M. *Langmuir* **2011**, *27*, 9105.

(14) (a) Shimano, S.; Zhou, H.; Honma, I. *Chem. Mater.* **2007**, *19*, 5216. (b) Lee, U.-H.; Kudo, T.; Honma, I. *Chem. Commun.* **2009**, 3068.

(15) Hanabusa, K.; Fukui, H.; Suzuki, M.; Shirai, H. *Langmuir* **2005**, *21*, 10383.

(16) (a) Kimizuka, N.; Nakashima, T. *Langmuir* **2001**, *17*, 6759. (b) Ikeda, A.; Sonoda, K.; Ayabe, M.; Tamaru, S.; Nakashima, T.; Kimizuka, N.; Shinkai, S. *Chem. Lett.* **2001**, 1154.

(17) (a) He, Y.; Lodge, T. P. *Chem Cmmun.* **2007**, 2732. (b) He, Y.; Lodge, T. P. *Macromolecules* **2008**, *41*, 167.

(18) (a) Lewandowski, A.; Świderska, A. *Solid State Ionics* **2003**, *161*, 243. (b) Isshiki, Y.; Nakamura, M.; Tabata, S.; Dokko, K.; Watanabe, M. *Polym. Adv. Tech.* **2011**, *22*, 1254.

(19) (a) Shobukawa, H.; Tokuda, H.; Susan, M.; Watanabe, M. *Electrochim. Acta* **2005**, *50*, 3872. (b) Shin, J.-H.; Henderson, W. A.; Passerini, S. *J. Electrochem. Soc.* **2005**, *152*, A978. (c) Ye, H.; Huang, J.; Xu, J. J.; Khalfan, A.; Greenbaum, S. G. *J. Electrochem. Soc.* **2007**, *154*, A1048.

(20) (a) Lee, S.-Y.; Yasuda, T.; Watanabe, M. *J. Power Sources* **2010**, *195*, 5909. (b) Lee, S.-Y.; Ogawa, A.; Kanno, M.; Nakamoto, H.; Yasuda, T.; Watanabe, M. *J. Am. Chem. Soc.* **2010**, *132*, 9764.

(21) (a) Wang, P.; Zakeeruddin, S. M.; Exnar, I.; Grätzel, M. *Chem. Commun.* **2002**, 2972. (b) Kawano, R.; Katakabe, T.; Shimosawa, H.; Nazeeruddin, M. K.; Grätzel, M.; Matsui, H.; Kitamura, T.; Tanabe, N.; Watanabe, M. *Phys. Chem. Chem. Phys.* **2010**, *12*, 1916.

(22) (a) Lu, W.; Fadeev, A. G.; Qi, E.; Smela, B. H.; Mattes, B. R.; Ding, J.; Spinks, G. M.; Mazurkiewicz, J.; Zhou, D. Z.; Wallace, G. G.; MacFarlane, D. R.; Forsyth, S. A.; Forsyth, M. *Science* **2002**, *297*, 983. (b) Zhou, D.; Spinks, G.; M. Wallace, G. G.; Tiyapiboonchaiya, C.; MacFarlane, D. R.; Forsyth, M.; Sun, J. *Electrochim. Acta* **2003**, *48*, 2355.

(23) (a) Bennett, M. D.; Leo, D. J. *Sens. Actuators A* **2004**, *115*, 79. (b) Akle, B. J.; Bennett, M. D.; Leo, D. J. *Sens. Actuators A* **2006**, *126*, 173.

(24) (a) Fukushima, T.; Asaka, K.; Kosaka, A.; Aida, T. *Angew. Chem., Int. Ed.* **2005**, *44*, 2410. (b) Mukai, K.; Asaka, K.; Kiyohara, K.; Sugino, T.; Takeuchi, I.; Fukushima, T.; Aida, T. *Electrochim. Acta* **2008**, *53*, 5555.

(25) (a) Bara, J. E.; Camper, D. E.; Gin, D. L.; Noble, R. D. *Acc. Chem. Res.* **2010**, *43*, 152. (b) Bara, J. E.; Hatakeyama, E. S.; Gabriel, C. J.; Zeng, X.; Lessmann, S.; Noble, R. D. *J. Membr. Sci.* **2008**, *316*, 186.

(26) Scott, K.; Basov, N.; Jachuck, R.; Winterton, N.; Cooper, A.; Davies, C. *Chem. Eng. Res. Des.* **2005**, *83*, 1179.
(27) (a) Lee, J.; Panzer, M. J.; He, Y.; Lodge, T. P.; Frisbie, C. D. *J. Am. Chem. Soc.* **2007**, *129*, 4532. (b) Cho, J. H.; Lee, J.; Xia, Y.; Kim, B.; He, Y.; Renn, M. J.; Lodge, T. P.; Frisbie, C. D. *Nat. Mater.* **2008**, *7*, 900. (c) Lee, J.; Kaake., L. G.; Cho, J. H.; Zhu, X.-Y.; Lodge, T. P.; Frisbie, C. D. *J. Phys. Chem. C* **2009**, *113*, 8972.
(28) *Electroactive Polymer (EAP) Actuators as Artificial Muscles*; Bar-Cohen, Y., Ed.; SPIE Press: Bellingham, WA, 2001.
(29) Pelrine, R.; Kombluh, R.; Pei, Q.; Joseph, J. *Science* **2000**, *287*, 836.
(30) (a) Asaka, K.; Oguro, K.; Nishimura, Y.; Mizuhata, M.; Takenaka, H. *Polym. J.* **1995**, *27*, 436. (b) Shahinpoor, M. *Electrochim. Acta* **2003**, *48*, 2343.
(31) (a) Kaneto, K.; Kaneko, M.; Min, Y.; MacDiarmid, A. G. *Synth. Met.* **1995**, *71*, 2211. (b) Baughman, R. H. *Synth. Met.* **1996**, *78*, 339. (c) Smela, E. *Adv. Mater.* **2003**, *15*, 48.
(32) Osada, Y.; Okuzaki, H.; Hori, H. *Nature* **1992**, *355*, 242.
(33) (a) Takeuchi, I.; Asaka, K.; Kiyohara, K.; Sugino, T.; Terasawa, N.; Mukai, K.; Shiraishi, S. *Carbon* **2009**, *47*, 1373. (b) Takeuchi, I.; Asaka, K.; Kiyohara, K.; Sugino, T.; Terasawa, N.; Mukai, K.; Fukushima, T.; Aida, T. *Electrochim. Acta* **2009**, *54*, 1762. (c) Terasawa, N.; Takeuchi, I.; Matsumoto, H. *Sens. Actuators, B* **2009**, *139*, 624. (d) Terasawa, N.; Takeuchi, I.; Matsumoto, H.; Mukai, K.; Asaka, K. *Sens. Actuators B* **2011**, *156*, 539. (e) Lee, J.-W.; Yoo, Y.-T. *Sens. Actuators B* **2009**, *137*, 539.
(34) (a) Wang, J.-S.; Matyjaszewski, K. *Macromolecules* **1995**, *28*, 7901. (b) Matyjaszewski, K.; Xia, J. *Chem. Rev.* **2001**, *101*, 2921. (c) Matyjaswewski, K.; Tsarevsky, N. V. *Nat. Chem.* **2009**, *1*, 276. (d) Tsarevsky, N. V.; Matyjaszewski, K. *Chem. Rev.* **2007**, *107*, 2270. (e) Patten, T. E.; Xia, J.; Abernathy, T.; Matyjaszewski, K. *Science* **1996**, *272*, 866.
(35) (a) Kato, M.; Kamigaito, M.; Sawamoto, M.; Higashimura, T. *Macromolecules* **1995**, *28*, 1721. (b) Kamigaito, M.; Ando, T.; Sawamoto, M. *Chem. Rev.* **2001**, *101*, 3689.
(36) Ueki, T.; Karino, T.; Kobayashi, Y.; Shibayama, M.; Watanabe, M. *J. Phys. Chem. B.* **2007**, *111*, 4750.
(37) Baughman, R. H.; Cui, C.; Zakhidov, A. A.; Iqbal, Z.; Barisci, J. N.; Spinks, G. M.; Wallace, G. G.; Mazzoldi, A.; Rossi, D. D.; Rinzler, A. G.; Jaschinski, O.; Roth, S.; Kertesz, M. *Science* **1999**, *284*, 1340.
(38) (a) Nanjo, S.; Watanabe, M.; Asai, K.; Yokoyama, K.; Yamamoto, M. *Abst. 71st Annu. Meet. Electrochem. Soc. Jpn.* **2004**, 263. (b) Okuno, T.; Sugoh, N.; Kato, T.; Ohgi, H.; Watanabe, M. *PCT Int. Appl.* WO2008123064, 2008.
(39) Bonhôte, P.; Dias, A.-P.; Papageorgiou, N.; Kalyanasundaram, K.; Grätzel, M. *Inorg. Chem.* **1996**, *35*, 1168.
(40) Karanam, S.; Goossens, H.; Klumperman, B.; Lemstra, P. *Macromolecules* **2003**, *36*, 3051.
(41) Santangelo, P. G.; Roland, C. M. *Macromolecules* **1998**, *31*, 4581.
(42) Mok, M. M.; Liu, X.; Bai, Z.; Lei, Y.; Lodge, T. P. *Macromolecules* **2011**, *44*, 1016.
(43) Bates, F. S. *Science* **1991**, *251*, 898.
(44) Jannasch, P. *Polymer* **2002**, *43*, 6449.
(45) (a) Tokuda, H.; Tsuzuki, S.; Susan, M. A. B. H.; Hayamizu, K.; Watanabe, M. *J. Phys. Chem. B* **2006**, *110*, 19593. (b) Ueno, K.; Tokuda, H.; Watanabe, M. *Phys. Chem. Chem. Phys.* **2010**, *12*, 1649.
(46) (a) Palmre, V.; Brandell, D.; Mäeorg, U.; Torop, J.; Volobujeva, O.; Punning, A.; Johanson, U.; Kruusmaa, M.; Aabloo, A. *Smart Mater. Struct.* **2009**, *18*, 095028. (b) Torop, J.; Palmre, V.; Arulepp, M.; Sugino, T.; Asaka, K.; Aabloo, A. *Carbon* **2011**, *49*, 3113. (c) Terasawa, N.; Takeuchi, I. *Sens. Actuators B* **2010**, *145*, 775.
(47) (a) Noda, A.; Hayamizu, K.; Watanabe, M. *J. Phys. Chem. B* **2001**, *105*, 4603. (b) Tokuda, H.; Hayamizu, K.; Ishii, K.; Susan, M. A. B. H.; Watanabe, M. *J. Phys. Chem B* **2004**, *108*, 16593. (c) Tokuda, H.; Hayamizu, K.; Ishii, K.; Susan, M. A. B. H.; Watanabe, M. *J. Phys. Chem B* **2005**, *109*, 6103. (d) Tokuda, H.; Ishii, K.; Susan, M. A. B. H.; Tsuzuki, S.; Hayamizu, K.; Watanabe, M. *J. Phys. Chem. B* **2006**, *110*, 2833. (e) Tsuzuki, S.; Shinoda, W.; Saito, H.; Mikami, M.; Tokuda, H.; Watanabe, M. *J. Phys. Chem. B* **2009**, *113*, 10641.
(48) Wang, C. S.; Zhang, X. B.; Yang, H. S.; Qi, Z. F.; He, P. M.; Li, W. Z. *J. Electrochem. Soc.* **1999**, *146*, 1696.

NOTE ADDED AFTER ASAP PUBLICATION

This article was published ASAP on December 15, 2001. Due to a production error, various revisions to Table 1, equations, and several places throughout the text were not present. The correct version posted on December 22, 2011.